



Published in final edited form as:

J Immunol. 2020 April 15; 204(8): 2277–2284. doi:10.4049/jimmunol.1701478.

Gut Microbiota Contributes to Spontaneous Colitis in E3 Ligase Itch-Deficient Mice

Mahesh Kathania^{*,†}, Elviche L. Tsakem^{*,†}, Arianne L. Theiss[‡], K. Venuprasad^{*,†}

^{*}Division of Digestive and Liver Diseases, Department of Internal Medicine, University of Texas Southwestern Medical Center, Dallas, TX 75390;

[†]Department of Immunology, University of Texas Southwestern Medical Center, Dallas, TX 75390;

[‡]Division of Gastroenterology and Hepatology, School of Medicine at the Anschutz Medical Campus, University of Colorado, Aurora, CO 80045

Abstract

Inflammatory bowel diseases are associated with complex shifts in microbiota composition. However, it remains unclear whether specific subsets of commensal bacteria induce inflammatory bowel diseases in genetically susceptible hosts. In this study, we found that deficiency of the E3 ligase Itch, which leads to spontaneous colitis and rectal prolapse, is associated with alteration of the gut microbiota. 16S rRNA sequencing showed expansion of colitogenic *Bacteroides* sp. in Itch^{-/-} mice. Treatment with broad-spectrum antibiotics substantially reduced colonic inflammation in Itch^{-/-} mice. Microbiota of Itch^{-/-} mice failed to induce spontaneous colitis upon transfer to Itch^{+/+} mice but aggravated chemically induced colitis. Furthermore, we found that *Bacteroides vulgatus*, which is expanded in Itch^{-/-} mice, was sufficient to induce colon inflammation in Itch^{-/-} mice.

The gastrointestinal tract is colonized by an extraordinarily large number of commensal microbes, within which *Bacteroidetes*, *Firmicutes*, and *Proteobacteria* are the dominant phyla (1, 2). The coexistence of resident commensals and a single layer of epithelial cells play a beneficial role in regulating both energy harvesting from nutrients and immune system function (3). A disturbance of this balanced state (dysbiosis) directly or indirectly contributes to persistent intestinal inflammation that manifests as the two distinct clinical entities of inflammatory bowel disease (IBD), Crohn disease, and ulcerative colitis (4–6). Therefore, determining the factors that regulate these complex host-commensal relationships and promote the development of colitis is of great clinical and scientific interest.

Posttranslational modification mediated by ubiquitin conjugation plays a crucial regulatory role in inflammation (7). Ubiquitination involves a cascade of biochemical reactions through ubiquitin-activating (E1) enzymes, ubiquitin-conjugating (E2) enzymes, and ubiquitin ligase

Address correspondence and reprint requests to Dr. K. Venuprasad, University of Texas Southwestern Medical Center, Dallas, TX 75390. venuprasad.poojary@utsouthwestern.edu.

The online version of this article contains supplemental material.

Disclosures

The authors have no financial conflicts of interest.

(E3) enzymes (7). The E3 ubiquitin ligases are critical components of this system because they recognize, bind to, and recruit specific target proteins for ubiquitination (7).

Itch is an E3 ubiquitin ligase that belongs to the HECT (homologous to the E6-AP C terminus) family. Itch contains a protein kinase C-related C2 domain, four WW domains (each of which contain two conserved tryptophan residues), and the HECT ligase domain (8). A truncated mutation of human Itch results in inflammatory disorders, including enteropathy (9). We have demonstrated recently that Itch deficiency in mice leads to spontaneous development of rectal prolapse because of severe colonic inflammation (10). In this study, we demonstrate that Itch plays a crucial role in regulation of gut microbiota and colonic inflammation.

Materials and Methods

Mice

C57BL/6J mice were originally obtained from Jackson Laboratory and bred in-house for more than 10 generations. These mice were then crossed with Itch^{-/-} mice and the resulting heterozygous mice were used as breeders. The littermate Itch^{+/+} and Itch^{-/-} mice from these breeders were used in this study. Itch^{-/-} mice have been described previously (10); Itch^{-/-}Rorc^{-/-} double knockout (DKO) mice were generated by crossing Itch^{-/-} with Rorc^{tm1Litt/J} mice (10). All mice were backcrossed at least 10 times with wild-type (WT) mice. All mice were fed irradiated food and maintained in autoclaved cages. Mice used in this study were age-matched, both females and males were used without observing differences between genders. In all experiments, up to five mice were housed per cage. Littermates were assigned to experimental groups according to genotype. All mice used in this study were bred and housed in individually ventilated cages in the same room of the specific pathogen-free facility with autoclaved food and bedding in the barrier facility at the Baylor Institute for Immunology Research and University of Texas Southwestern Medical Center. All experiments were performed in accordance with the guidelines of the Institutional Animal Care and Use Committee of Baylor Research Institute and University of Texas Southwestern Medical Center.

16S rRNA gene sequencing

16S rRNA gene sequencing was performed on fecal pellets from Itch^{+/+} and littermate Itch^{-/-} collected at 8 wk. In brief, the 16S rRNA gene V4 V region PCR primers 515/806 (11) were used in a single-step 30-cycle PCR using the HotStarTaq Plus Master Mix Kit (Qiagen, Hilden, Germany) under the following conditions: 94°C for 3 min, followed by 28 cycles (five cycles used on PCR products) of 94°C for 30 s, 53°C for 40 s, and 72°C for 1 min, after which a final elongation step at 72°C for 5 min was performed. Sequencing was performed at MR DNA (Shallowater, TX) on an Ion Torrent Personal Genome Machine following the manufacturer's guidelines. Sequence data were processed using a proprietary analysis pipeline (MR DNA). In summary, sequences were depleted of barcodes and primers and then sequences <150 bp were removed; sequences with ambiguous base calls and with homopolymer runs exceeding 6 bp were also removed. Sequences were denoised, operational taxonomic units (OTUs) were generated, and chimeras were removed. OTUs

were defined by clustering at 3% divergence (97% similarity). Final OTUs were taxonomically classified using BLASTn against a curated database derived from GreenGenes, Ribosomal Database Project-II, and National Center of Biotechnology Information (12). The raw data for 16s rRNA gene sequencing have been deposited to the National Center for Biotechnology Information Sequence Read Archive database (Sequence Read Archive accession: PRJNA605559).

Antibiotic treatment and *Bacteroides* reconstitution

The gut microbiota of 8-wk-old C57BL/6 mice was depleted by feeding a mixture of antibiotics in drinking water ad libitum for 4 wk. In brief, mice were provided 1 g/l ampicillin, 500 mg/l vancomycin, 1 g/l neomycin sulfate, and 1 g/l metronidazole in drinking water, as previously described (13). *Bacteroides* strains *Bacteroides uniformis* (ATCC 8492), *Bacteroides caccae* (ATCC 43185), *Parabacteroides goldsteinii* (ATCC BAA-1180), *Bacteroides ovatus* (ATCC 8483), and *Bacteroides vulgatus* (ATCC 8482) were purchased from American Type Culture Collection (Manassas, VA). *Bacteroides* strains were cultured in BBL Chopped Meat Carbohydrate Broth, Pre-Reduced II (BD Biosciences, Sparks, MD). Antibiotic-pretreated Itch^{-/-} mice were gavaged 1×10^8 CFU per mouse, and mice were sacrificed after 4 wk.

Fecal transplantation and bacterial culture administration

The gut microbiota of 8-wk-old Itch^{+/+} mice was first depleted using antibiotics in their drinking water for 4 wk. For fecal transplant, fecal pellets from untreated Itch^{-/-} mice were resuspended in PBS (one fecal pellet per 1 ml of PBS). A total of 200 μ l of the resuspended pool fecal material was given by gavage to mice over 3 consecutive d, starting 1 d after the antibiotic treatment was stopped and then every week for 3 wk (14). Itch^{+/+} mice were then sacrificed after 12 wk of fecal transplant. The Itch^{+/+} mice that received microbiota of Itch^{-/-} mice were ~6-mo-old at the end of experiment.

RT-PCR analysis

Total RNA was prepared using RNeasy Mini Kit (Qiagen) followed by cDNA synthesis using the Verso cDNA Kit (Thermo Fisher Scientific, Richardson, TX). Quantitative RT-PCR was performed on a Master-cycler Realplex (Eppendorf, Hamburg, Germany). A Light Cycler 480 SYBR Green I Master Reaction Mix (Roche, Basel, Switzerland) was used in a 20- μ l reaction volume. The expression of individual genes was normalized to the expression of actin. Cycling conditions were 95°C for 2 min, followed by 50 cycles of 95°C for 15 s, 55°C for 15 s, and 72°C for 20 s.

Fecal bacterial DNA extraction

Bacterial fecal DNA was extracted using a commercial kit (QIAamp DNA Stool Mini Kit; Qiagen, Valencia, CA) following the manufacturer's recommendations. Extracted genomic DNA was used as a template for PCR amplification of different bacterial species.

Dextran sulfate sodium–induced colitis

Acute colitis was induced with 2.5% (w/v) dextran sulfate sodium (DSS) (molecular mass 36–50 kDa; MP Biologicals, Solon, OH) dissolved in sterile, distilled water ad libitum for 5 d followed by normal drinking water for 3 d. Fresh DSS solution was provided on day 3. Mice were sacrificed on day 8. Scoring for stool consistency and occult blood was done as previously described (15). Briefly, stool scores were determined as follows: 0 = well-formed pellets, 2 = semiformal stools, and 4 = liquid stool that adhered to the anus. Bleeding scores were determined as follows: 0 = no blood, 2 = visible blood traces in stool, and 4 = gross rectal bleeding. Stool consistency scores and bleeding scores were added and presented as clinical scores.

Histopathology

Colons from *Itch*^{+/+} and *Itch*^{-/-} were fixed in formalin and embedded in paraffin, and tissue sections (5 μ m) were stained with H&E and blindly scored. Histopathological evaluation of the entire section was performed by determining the crypt distortion, inflammation, presence of the immune cell infiltration in intestine mucosa, and infiltration degree of immune cell in submucosa. Histology scores were determined as follows: 0 = no architectural changes, 1 = inflammatory infiltrate, 2 = lamina propria neutrophils and eosinophils, 3 = neutrophils in epithelium, 4 = crypt destruction, and 5 = erosions or ulceration.

Statistical analysis

For data with normal distribution, one-way ANOVA was performed. Differences between two groups were evaluated using an unpaired Student *t* test. The data are presented as the mean \pm SD, and differences were considered statistically significant at *p* < 0.05. GraphPad Prism statistical software (version 5.0; GraphPad Software, La Jolla, CA) was used for analyses.

Results

Gut microbiota is altered in *Itch*^{-/-} mice

We reported recently that *Itch* negatively regulates IL-17 expression in the colonic mucosa by targeting ROR- γ t for ubiquitination. *Itch*^{-/-} mice spontaneously develop rectal prolapse because of severe colonic inflammation (10). Because emerging evidence suggests an intimate link between dysbiotic gut microflora and IL-17 in colon inflammation (16–18), we analyzed the microbiota composition of fecal pellets by 16S rRNA sequencing of the V4 region. The microbial compositions of *Itch*^{+/+} and *Itch*^{-/-} mice were assessed using UniFrac, a phylogeny-based measure of the degree of similarity between microbial communities. Pairwise distances were determined for all pairs of samples based on the taxonomic representation (unweighted). Principal coordinate analysis based on the UniFrac distances was used to visualize the differences among samples.

We found that the *Itch*^{-/-} mice hosted a significantly distinct bacterial population compared with littermate *Itch*^{+/+} control mice (Fig. 1A, 1B). Shannon and OTU rarefaction curves reached stable values, showing that the depth of sequencing would include most species found in the samples (Supplemental Fig. 1A, 1B). *Itch*^{+/+} mice had much less α diversity

than *Itch*^{-/-} mice as measured by the Shannon index (Supplemental Fig. 1C). Taxon-based analysis revealed that *Itch*^{-/-} mice showed increased *Bacteroidetes*, whereas *Itch*^{+/+} mice exhibited a higher *Firmicutes*-to-*Bacteroidetes* ratio (Fig. 1C, 1D). Taxonomic abundance was influenced in *Itch*^{-/-} mice at multiple levels. Several species of the Bacteroidaceae, Prevotellaceae, Streptococcaceae, and Rikenellaceae families were increased in relative abundance in *Itch*^{-/-} mice, whereas the percentage of Bifidobacteriaceae family members were reduced (Fig. 1E). *B. uniformis*, *B. caccae*, *P. goldsteinii*, *B. ovatus*, and *B. vulgatus* were increased in *Itch*^{-/-} mice (Fig. 1F). Fecal DNA PCR was performed to confirm the presence of the above species (Supplemental Fig. 2A). An age dependent change in microbiota of WT and *Itch*^{-/-} mice was performed by fecal DNA PCR. *Itch*^{-/-} mice started to show microbiota change at an early age compared with WT mice (Supplemental Fig. 2B). These data suggest an alteration in the gut microbiota of *Itch*^{-/-} mice.

Broad-spectrum antibiotic treatment alleviates spontaneous colonic inflammation in *Itch*^{-/-} mice

To determine if the commensal microbes of *Itch*^{-/-} mice trigger colonic inflammation, we tested whether broad-spectrum antibiotic treatment would limit the development of spontaneous colitis. For this, we depleted the microbiota of *Itch*^{-/-} mice by 4 wk of oral administration of vancomycin, neomycin, metronidazole, and ampicillin (19). Mice were sacrificed 5 wk after antibiotic treatment. Histological examination of colon sections showed reduced colon inflammation in the *Itch*^{-/-} mice treated with antibiotics compared with age-matched untreated *Itch*^{-/-} mice (Fig. 2A).

Because we demonstrated that deficiency of *Itch* leads to elevated IL-17 expression in the colonic mucosa (10), we analyzed the level of IL-17 expression in antibiotic-treated mice by RT-PCR experiments. As expected, the levels of IL-17A and IL-17F were significantly reduced in the antibiotic-treated mice compared with control untreated mice (Fig. 2B).

Because IL-17 promotes the inflammatory response by inducing multiple cytokines, chemokines, and matrix metalloproteinases (MMPs) (20), we analyzed the expression of genes encoding IL-17-induced chemokines and MMPs. Our results showed that antibiotic treatment substantially reduced the expression of CXCL1, CCL2, CCL7, CCL20, MMP1, MMP2, MMP3, and MMP13 mRNA in *Itch*^{-/-} colons (Fig. 2C, 2D). These results suggest that the commensal microbiota contribute to spontaneous colitis in *Itch*^{-/-} mice.

Reconstitution of *Itch*^{-/-} microbiota in *Itch*^{+/+} mice does not induce spontaneous colon inflammation

It has been shown that the microbiota of the mice that are genetically susceptible to develop colitis [e.g., T-bet^{-/-} Rag2^{-/-} (TRUC) mice (19), NLRP6^{-/-} mice (21, 22), and NOD2^{-/-} mice (23)] is transferable and induces severe colitis in WT mice upon cohousing. To test if the *Itch*^{-/-} microbiota was transferable and induced colitis in WT mice, we treated WT mice with antibiotics to deplete the resident microbiota. *Itch*^{-/-} fecal pellets were reconstituted in PBS, and 200 µl of the resuspended fecal sample was given by gavage to antibiotic-pretreated mice. This was repeated for 3 consecutive d, starting 1 d after the antibiotic treatment was stopped. Four weeks after the final gavage, fecal pellets were collected from

the *Itch*^{-/-} microbiota-recipient *Itch*^{+/+} mice. 16S rRNA sequencing showed that *Itch*^{+/+} mice were reconstituted with *Itch*^{-/-} microbiota (Fig. 3A, 3B). To examine the dissimilarity between microbiota, we measured the Yue and Clayton (ΘYC) distances. There was increased variation in microbiota of WT (*Itch*^{+/+}) with *Itch*^{-/-} mice. Increased variation was also seen in microbiota of WT mice compared with WT mice gavaged with *Itch*^{-/-} microbiota. There was much less variation between microbiota of *Itch*^{-/-} mice and WT mice gavaged with *Itch*^{-/-} microbiota as seen by ΘYC distances (Fig. 3C). Shannon and OTU rarefaction curves reached stable values, showing that the depth of sequencing included most species found in the samples (Supplemental Fig. 3A, 3B). *Itch*^{+/+} mice had less α diversity than *Itch*^{+/+} mice given *Itch*^{-/-} microbiota as measured by Shannon index (Supplemental Fig. 3C).

To investigate if the *Itch*^{-/-} microbiota induced colonic inflammation in *Itch*^{+/+} mice, we monitored body weight change and diarrhea in the recipient mice. Unexpectedly, no significant change in either body weight or diarrhea incidence was observed (data not shown). Similarly, histological examination showed neither signs of inflammatory infiltration nor any morphological changes (Fig. 3D, 3E). Additionally, the level of colitogenic cytokines such as TNF, IL-16, IL-1β, and IL-17 were similar to control mice (Fig. 3F, 3G). These data suggest that the colitis observed in *Itch*^{-/-} mice is not transferable via its microbiota.

Reconstitution of *Itch*^{-/-} microbiota in *Itch*^{+/+} mice aggravates DSS-induced colitis

Next, we tested if the *Itch*^{-/-} microbiota affected chemically induced colitis in WT mice. We reconstituted antibiotic-pretreated WT mice with *Itch*^{-/-} microbiota via oral gavage. These mice were then treated with 2.5% (w/v) DSS dissolved in sterile, distilled water ad libitum for 5 d followed by normal drinking water for 3 d. Body weight change, diarrhea score, and fecal occult blood (FOB) scores were monitored. As shown in Fig. 4A–C, *Itch*^{+/+} mice reconstituted with *Itch*^{-/-} microbiota showed increased body weight loss, higher diarrhea score, and higher FOB score compared with *Itch*^{+/+} control mice. *Itch*^{-/-} mice showed significantly higher scores than both *Itch*^{+/+} mice reconstituted with *Itch*^{-/-} microbiota and *Itch*^{+/+} control mice. Histological examination of colon sections after DSS treatment also showed increased histology scores in *Itch*^{+/+} mice reconstituted with *Itch*^{-/-} microbiota (Fig. 4D), suggesting severe colitis.

Microbiota of *Itch*^{-/-}*Rorc*^{-/-} DKO mice are similar to *Itch*^{-/-} mice

We reported earlier that aged (6- to 8-mo-old) *Itch*^{-/-} mice spontaneously develop rectal prolapse because of severe colonic inflammation. Mechanistically, we demonstrated that *Itch* targets ROR-γt for ubiquitination and the defect in this regulatory mechanism in *Itch*^{-/-} mice resulted in elevated IL-17 levels in colonic mucosa. To investigate if the elevated IL-17 leads to altered microbiota in *Itch*^{-/-} mice, we analyzed the microbiota composition of fecal pellets of *Itch*^{-/-} *Rorc*^{-/-} DKO mice. We found that the *Itch*^{-/-} and *Itch*^{-/-} *Rorc*^{-/-} DKO mice hosted a significantly distinct bacterial population compared with littermate WT and *Rorc*^{-/-} control mice (Fig. 5A, 5B). Taxon-based analysis showed that *Itch*^{-/-} *Rorc*^{-/-} DKO mice exhibited increased *Bacteroidetes* similar to that of *Itch*^{-/-} mice (Fig. 5B, 5C). WT

mice exhibited a higher *Firmicutes*-to-*Bacteroidetes* ratio similar to that of *Rorc*^{-/-} mice (Fig. 5D).

***B. vulgatus* induces colon inflammation in *Itch*^{-/-} mice**

Because the Bacteroidaceae family was expanded in the microbiota of *Itch*^{-/-} mice, we hypothesized that some member of this family triggers colitis in *Itch*^{-/-} mice. To test this, we gavaged five species (*B. uniformis*, *B. caccae*, *P. goldsteinii*, *B. ovatus*, and *B. vulgatus*) in antibiotic-pretreated *Itch*^{-/-} mice as described before (24). Only in mice inoculated with *B. vulgatus* did we observe body weight loss (Fig. 6A), decreased colon length (Fig. 6B), and, in histological examinations, increased crypt loss and infiltration of mononuclear cells (Fig. 6C, 6D). Mild inflammation was also observed in mice inoculated with *P. goldsteinii* (Fig. 6C, 6D).

Because we had shown that the colonic inflammation in *Itch*^{-/-} mice is driven by IL-17, we measured the level of IL-17 using the colon explant cultures. Our results showed increased levels of IL-17A only in mice gavaged with *B. vulgatus* (Fig. 6E). Similar results were obtained in RT-PCR experiments using the mRNA isolated from colon tissue of *Itch*^{-/-} with *B. vulgatus* (Fig. 6F). These results suggest that *B. vulgatus* is sufficient to induce colon inflammation in *Itch*^{-/-} mice.

Discussion

Instability in the composition of the gut bacterial communities has been linked to IBDs (3). However, whether a specific commensal bacterial subset induces IBD and, if so, whether its proportions in the microbiota are altered during disease remains unclear. Also, the role of commensal bacteria in the context of specific host genotypes remains unclear. In this study, we demonstrate that *Itch* deficiency leads to expansion of colitogenic *Bacteroides* sp., which was associated with spontaneous colitis. Thus, our results demonstrate that *Itch* has an essential role in shaping a protective assembly of gut bacterial communities and suggest that manipulation of dysbiosis is a potential therapeutic approach in the treatment of IBDs.

Intestinal *Bacteroides* are among the most abundant members of the commensal microbiota (25). They benefit the host through breakdown of complex dietary carbohydrates and modulation of mucosal glycosylation, gene expression, angiogenesis, and immune maturation (26). However, in genetically susceptible hosts, some *Bacteroides* sp. induce colitis (24, 25). We found that inoculation of antibiotic-treated *Itch*^{-/-} mice but not WT mice with *B. vulgatus* induced colonic inflammation. Our results are in line with previous reports that show that *B. vulgatus* induces colitis in *IL-10*^{-/-} *TGF-β*^{-/-} (DKO) mice (24) and in germ-free rats transgenically expressing HLA-B27 (27). It was shown that human enterotoxigenic *B. fragilis* induces colitis and promotes colon cancer growth in susceptible mice (28). However, we did not find *B. fragilis* colonization in *Itch*^{-/-} mice. It needs to be determined whether *B. fragilis* could induce colitis in *Itch*^{-/-} mice.

Genetic deletion of T-bet, Nod2, angiotensin-converting enzyme-2 (ACE2), and NLRP6 results in the emergence of transmissible, disease-predisposing commensals (19). However, the microbiota of *Itch*^{-/-} mice failed to induce colitis in WT type mice but significantly

enhanced chemically induced colitis. This genotype-dependent disparity in disease induction could be due to differences in host response.

Whether the altered microbiota is the cause or consequence of colonic inflammation in *Itch*^{-/-} mice remains unclear. Although it can be argued that the observed changes in the gut microbiota are due to differences in the inflammatory state, the observation that a pure culture of *B. vulgatus* that was expanded in *Itch*^{-/-} was sufficient to induce colitis suggests that the altered gut microbiota contributes to spontaneous colitis in *Itch*^{-/-} mice. Further, *Itch*^{-/-} *RORC*^{-/-} mice exhibited microbial composition similar to *Itch*^{-/-} mice suggesting that the alteration in the microbiota is independent of IL-17–driven inflammation. One possibility for alterations in the microbial community in *Itch*^{-/-} mice could be due to changes in secretory mucins by the gut epithelial cells. In support of this possibility, we found low expression of MUC2 in the colonic mucosa of *Itch*^{-/-} mice (Supplemental Fig. 4). Further, detailed analysis using epithelial cell–specific conditional knockout mice using gnotobiotic conditions would be necessary to fully elucidate the function of *Itch* in regulation of microbiota and colonic inflammation. Additionally, whether the alteration in the microbial composition observed in IBD patients is linked to defective *Itch* function in IBD patients (29) remains to be investigated. Nevertheless, this study highlights a novel, to our knowledge, function for the ubiquitin pathway in regulation of gut microbiota, which will open new avenues for exploration of this pathway. A clear understanding of the mechanism by which the gut mucosa discriminates between disease-predisposing microorganisms and mutualists could provide insights into disease onset in genetically predisposed individuals.

Supplementary Material

Refer to Web version on PubMed Central for supplementary material.

Acknowledgments

We thank Dr. Ezra Burstein for helpful discussions and Dr. Wayne Lancaster for critical reading of the manuscript.

This work was supported by grants from the National Institutes of Health (R01-DK115668-01), the Cancer Prevention Research Institute of Texas (RP160577), Baylor Charles A. Sammons Cancer Center and Baylor Scott and White Research Institute-Translational Genomics Research Institute collaborative grants (to K.V.), and Grant R01-DK117001 from the National Institutes of Health (to A.L.T.).

Abbreviations used in this article:

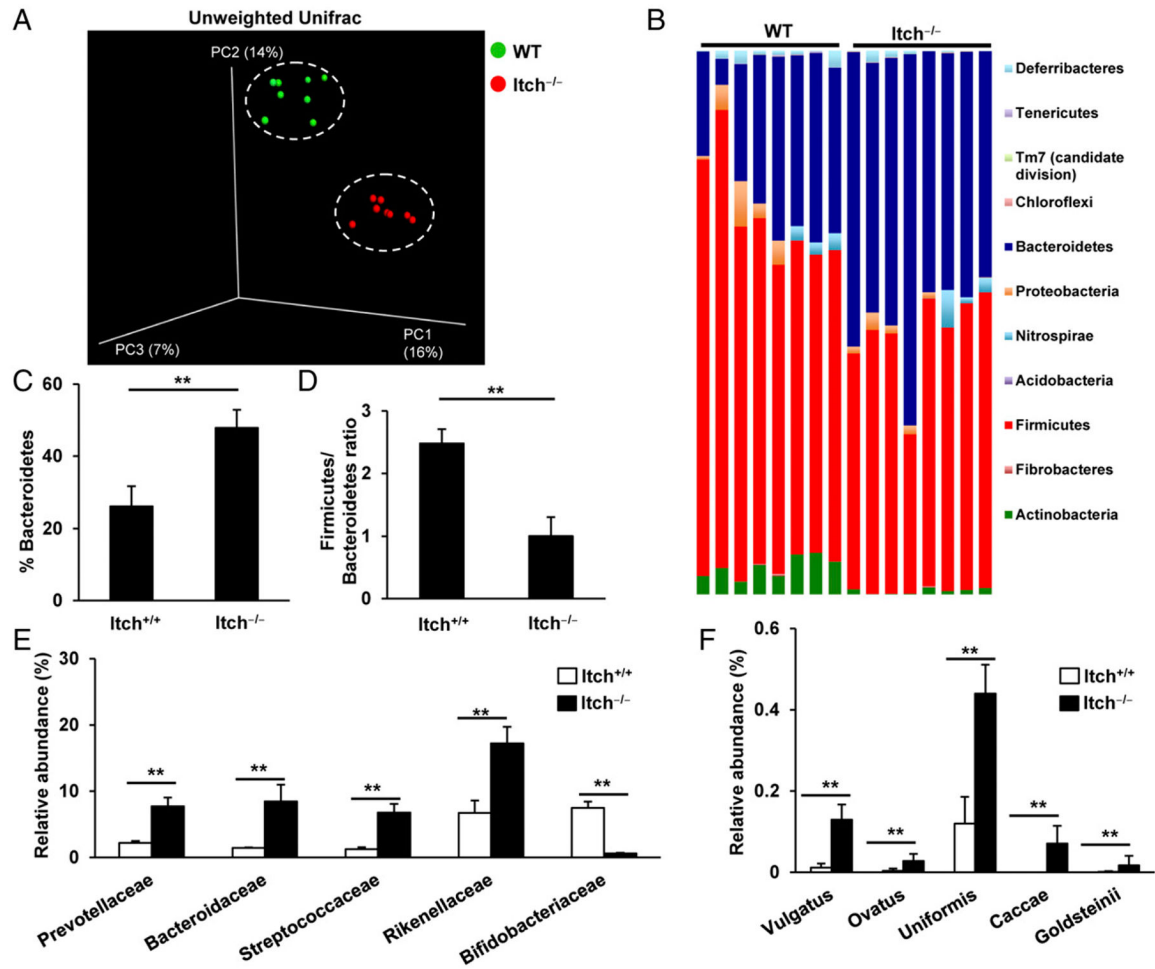
DKO	double knockout
DSS	dextran sulfate sodium
FOB	fecal occult blood
IBD	inflammatory bowel disease
MMP	matrix metalloproteinase
OTU	operational taxonomic unit

WT	wild-type
⊖YC	Yue and Clayton

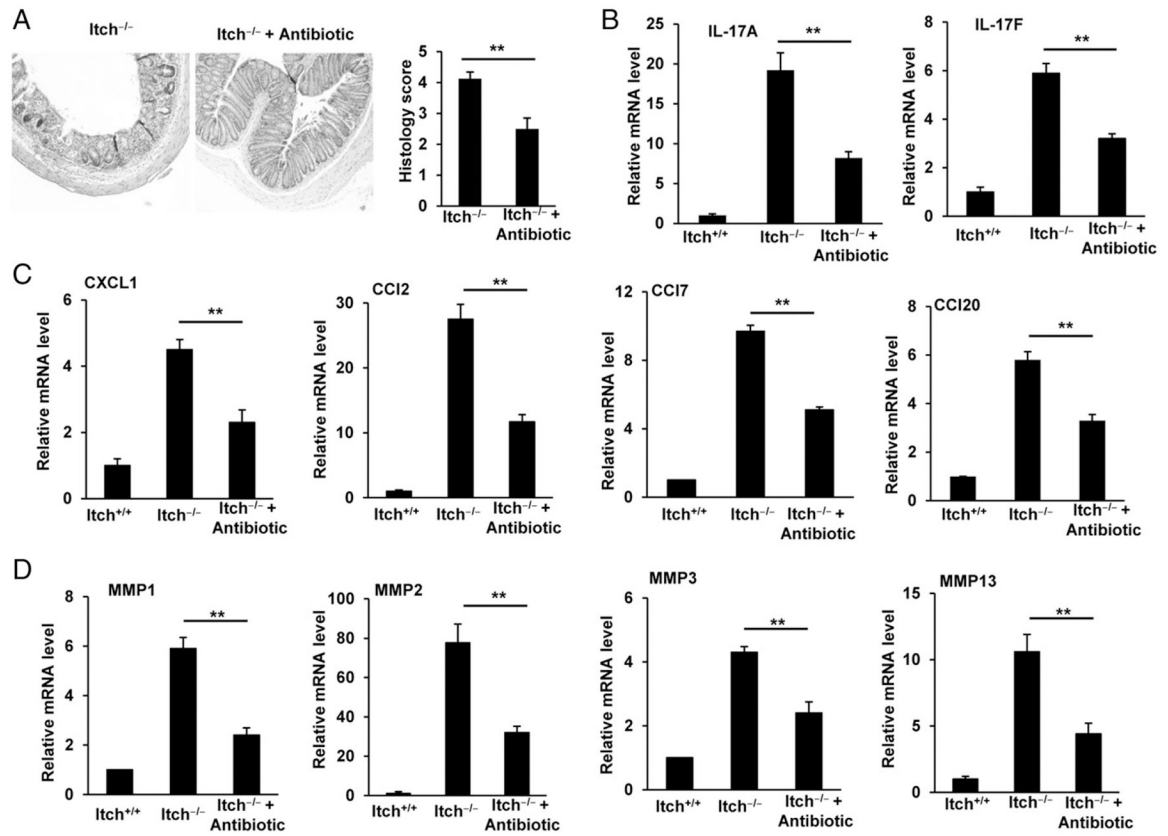
References

1. Ley RE, Hamady M, Lozupone C, Turnbaugh PJ, Ramey RR, Bircher JS, Schlegel ML, Tucker TA, Schrenzel MD, Knight R, and Gordon JI. 2008 Evolution of mammals and their gut microbes. *Science* 320: 1647–1651. [PubMed: 18497261]
2. Tilg H, Adolph TE, Gerner RR, and Moschen AR. 2018 The intestinal microbiota in colorectal cancer. *Cancer Cell* 33: 954–964. [PubMed: 29657127]
3. Garrett WS, Gordon JI, and Glimcher LH. 2010 Homeostasis and inflammation in the intestine. *Cell* 140: 859–870. [PubMed: 20303876]
4. Abraham C, and Cho JH. 2009 Inflammatory bowel disease. *N. Engl. J. Med* 361: 2066–2078. [PubMed: 19923578]
5. Gevers D, Kugathasan S, Denson LA, Vázquez-Baeza Y, Van Treuren W, Ren B, Schwager E, Knights D, Song SJ, Yassour M, et al. 2014 The treatment-naïve microbiome in new-onset Crohn's disease. *Cell Host Microbe* 15: 382–392. [PubMed: 24629344]
6. Knights D, Lassen KG, and Xavier RJ. 2013 Advances in inflammatory bowel disease pathogenesis: linking host genetics and the microbiome. *Gut* 62: 1505–1510. [PubMed: 24037875]
7. Hershko A, and Ciechanover A. 1998 The ubiquitin system. *Annu. Rev. Biochem* 67: 425–479. [PubMed: 9759494]
8. Venuprasad K, Zeng M, Baughan SL, and Massoumi R. 2015 Multifaceted role of the ubiquitin ligase Itch in immune regulation. *Immunol. Cell Biol* 93: 452–460. [PubMed: 25582340]
9. Lohr NJ, Molleston JP, Strauss KA, Torres-Martinez W, Sherman EA, Squires RH, Rider NL, Chikwava KR, Cummings OW, Morton DH, and Puffenberger EG. 2010 Human ITCH E3 ubiquitin ligase deficiency causes syndromic multisystem autoimmune disease. *Am. J. Hum. Genet* 86: 447–453. [PubMed: 20170897]
10. Kathania M, Khare P, Zeng M, Cantarel B, Zhang H, Ueno H, and Venuprasad K. 2016 Itch inhibits IL-17-mediated colon inflammation and tumorigenesis by ROR- γ t ubiquitination. *Nat. Immunol* 17: 997–1004. [PubMed: 27322655]
11. Caporaso JG, Lauber CL, Walters WA, Berg-Lyons D, Lozupone CA, Turnbaugh PJ, Fierer N, and Knight R. 2011 Global patterns of 16S rRNA diversity at a depth of millions of sequences per sample. *Proc. Natl. Acad. Sci. USA* 108(Suppl. 1): 4516–4522. [PubMed: 20534432]
12. DeSantis TZ, Hugenholtz P, Larsen N, Rojas M, Brodie EL, Keller K, Huber T, Dalevi D, Hu P, and Andersen GL. 2006 Greengenes, a chimera-checked 16S rRNA gene database and workbench compatible with ARB. *Appl. Environ. Microbiol* 72: 5069–5072. [PubMed: 16820507]
13. Rakoff-Nahoum S, Paglino J, Eslami-Varzaneh F, Edberg S, and Medzhitov R. 2004 Recognition of commensal microflora by toll-like receptors is required for intestinal homeostasis. *Cell* 118: 229–241. [PubMed: 15260992]
14. Ubeda C, Bucci V, Caballero S, Djukovic A, Toussaint NC, Equinda M, Lipuma L, Ling L, Gobourne A, No D, et al. 2013 Intestinal microbiota containing *Barnesiella* species cures vancomycin-resistant *Enterococcus faecium* colonization. *Infect. Immun* 81: 965–973. [PubMed: 23319552]
15. Zaki MH, Vogel P, Malireddi RK, Body-Malapel M, Anand PK, Bertin J, Green DR, Lamkanfi M, and Kanneganti TD. 2011 The NOD-like receptor NLRP12 attenuates colon inflammation and tumorigenesis. *Cancer Cell* 20: 649–660. [PubMed: 22094258]
16. Arthur JC, and Jobin C. 2011 The struggle within: microbial influences on colorectal cancer. *Inflamm. Bowel Dis* 17: 396–409. [PubMed: 20848537]
17. Elinav E, Nowarski R, Thaïss CA, Hu B, Jin C, and Flavell RA. 2013 Inflammation-induced cancer: crosstalk between tumours, immune cells and microorganisms. *Nat. Rev. Cancer* 13: 759–771. [PubMed: 24154716]
18. Gagliani N, Hu B, Huber S, Elinav E, and Flavell RA. 2014 The fire within: microbes inflame tumors. *Cell* 157: 776–783. [PubMed: 24813605]

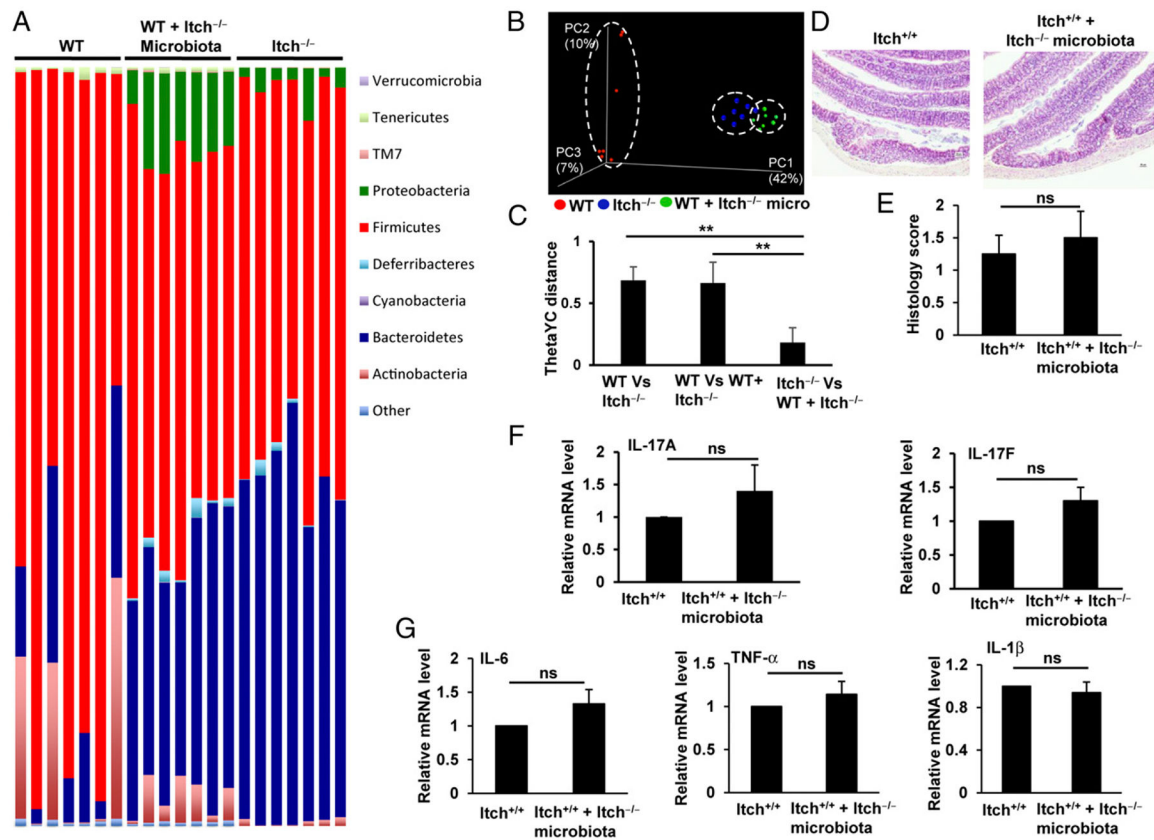
19. Garrett WS, Lord GM, Punit S, Lugo-Villarino G, Mazmanian SK, Ito S, Glickman JN, and Glimcher LH. 2007 Communicable ulcerative colitis induced by T-bet deficiency in the innate immune system. *Cell* 131: 33–45. [PubMed: 17923086]
20. Dong C 2008 TH17 cells in development: an updated view of their molecular identity and genetic programming. *Nat. Rev. Immunol* 8: 337–348. [PubMed: 18408735]
21. Elinav E, Strowig T, Kau AL, Henao-Mejia J, Thaiss CA, Booth CJ, Peaper DR, Bertin J, Eisenbarth SC, Gordon JI, and Flavell RA. 2011 NLRP6 inflammasome regulates colonic microbial ecology and risk for colitis. *Cell* 145: 745–757. [PubMed: 21565393]
22. Hu B, Elinav E, Huber S, Strowig T, Hao L, Hafemann A, Jin C, Wunderlich C, Wunderlich T, Eisenbarth SC, and Flavell RA. 2013 Microbiota-induced activation of epithelial IL-6 signaling links inflammasome-driven inflammation with transmissible cancer. [Published erratum appears in 2013 *Proc. Natl. Acad. Sci. USA* 110: 12852.] *Proc. Natl. Acad. Sci. USA* 110: 9862–9867. [PubMed: 23696660]
23. Couturier-Maillard A, Secher T, Rehman A, Normand S, De Arcangelis A, Haesler R, Huot L, Grandjean T, Bressenot A, Delanoye-Crespin A, et al. 2013 NOD2-mediated dysbiosis predisposes mice to transmissible colitis and colorectal cancer. *J. Clin. Invest* 123: 700–711. [PubMed: 23281400]
24. Bloom SM, Bijanki VN, Nava GM, Sun L, Malvin NP, Donermeyer DL, Dunne WM Jr., Allen PM, and Stappenbeck TS. 2011 Commensal *Bacteroides* species induce colitis in host-genotype-specific fashion in a mouse model of inflammatory bowel disease. *Cell Host Microbe* 9: 390–403. [PubMed: 21575910]
25. Wexler AG, and Goodman AL. 2017 An insider's perspective: *Bacteroides* as a window into the microbiome. *Nat. Microbiol* 2: 17026. [PubMed: 28440278]
26. Kau AL, Ahern PP, Griffin NW, Goodman AL, and Gordon JI. 2011 Human nutrition, the gut microbiome and the immune system. *Nature* 474: 327–336. [PubMed: 21677749]
27. Brakenhoff LK, van der Heijde DM, Hommes DW, Huizinga TW, and Fidder HH. 2010 The joint-gut axis in inflammatory bowel diseases. *J. Crohn's Colitis* 4: 257–268. [PubMed: 21122514]
28. Wu S, Rhee KJ, Albesiano E, Rabizadeh S, Wu X, Yen HR, Huso DL, Brancati FL, Wick E, McAllister F, et al. 2009 A human colonic commensal promotes colon tumorigenesis via activation of T helper type 17 T cell responses. *Nat. Med* 15: 1016–1022. [PubMed: 19701202]
29. Paul J, Singh AK, Kathania M, Elviche TL, Zeng M, Basrur V, Theiss AL, and Venuprasad K. 2018 IL-17-driven intestinal fibrosis is inhibited by Itch-mediated ubiquitination of HIC-5. *Mucosal Immunol.* 11: 427–436. [PubMed: 28612841]

**FIGURE 1.**

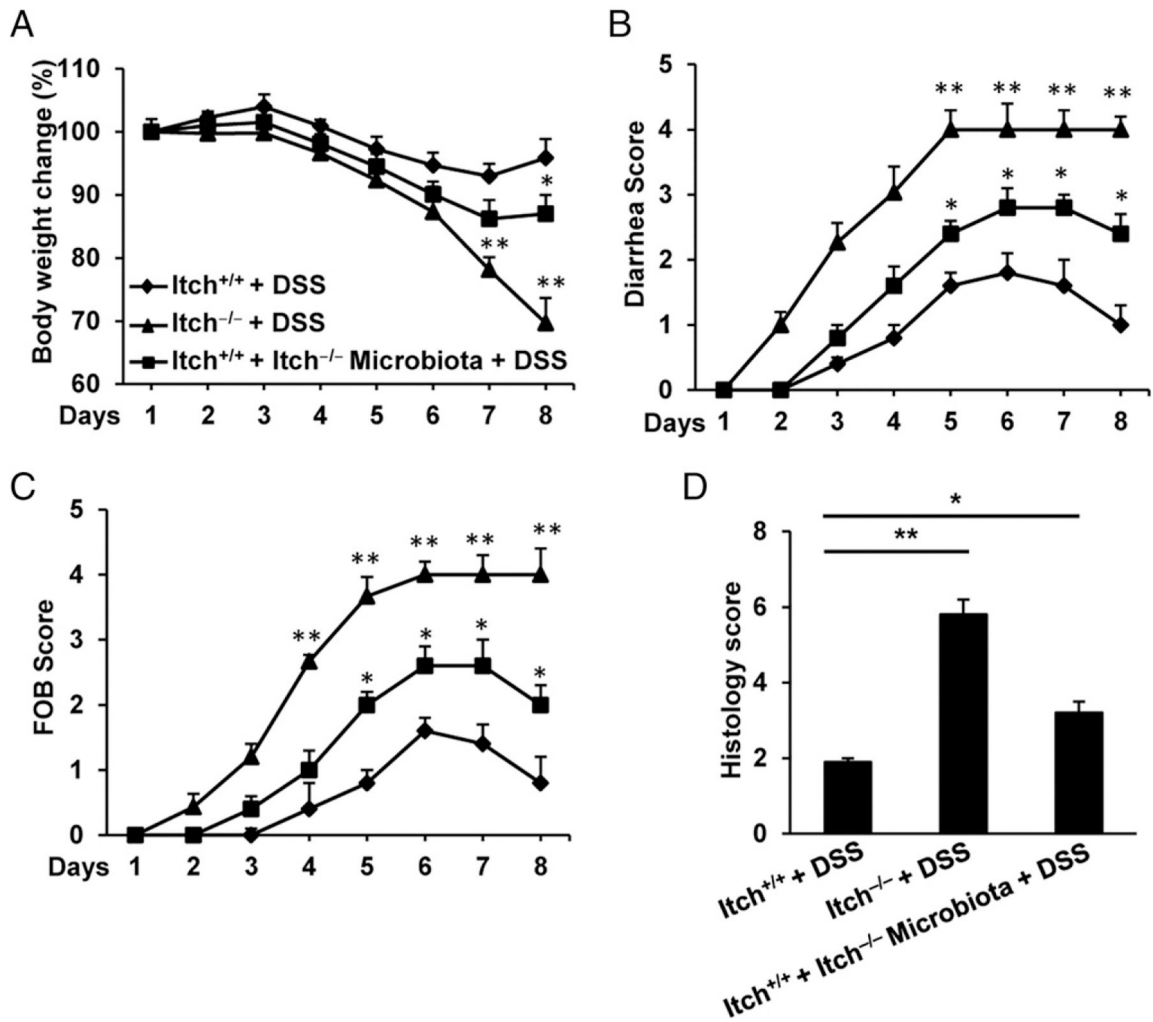
Itch^{-/-} mice have altered gut microbiota. Results from 16S rRNA sequencing of fecal pellets from *Itch*^{+/+} and *Itch*^{-/-} mice, showing (A) unweighted UniFrac distance principal coordinate analysis of the fecal microbiota from 8 *Itch*^{+/+} (green dots) and 8 *Itch*^{-/-} (red dots), (B) relative abundance of phylum-classified fecal microbiota, (C) percentage of *Bacteroidetes* present in fecal microbiota from *Itch*^{+/+} and *Itch*^{-/-} mice, (D) *Bacteroidetes*-to-*Firmicutes* ratio in fecal microbiota from *Itch*^{+/+} and *Itch*^{-/-} mice, and (E) percentage change in family level in fecal microbiota from *Itch*^{+/+} and *Itch*^{-/-} mice. (F) Percentage change in species level in fecal microbiota from *Itch*^{+/+} and *Itch*^{-/-} mice. Data represent mean ± SD. ***p* < 0.01.

**FIGURE 2.**

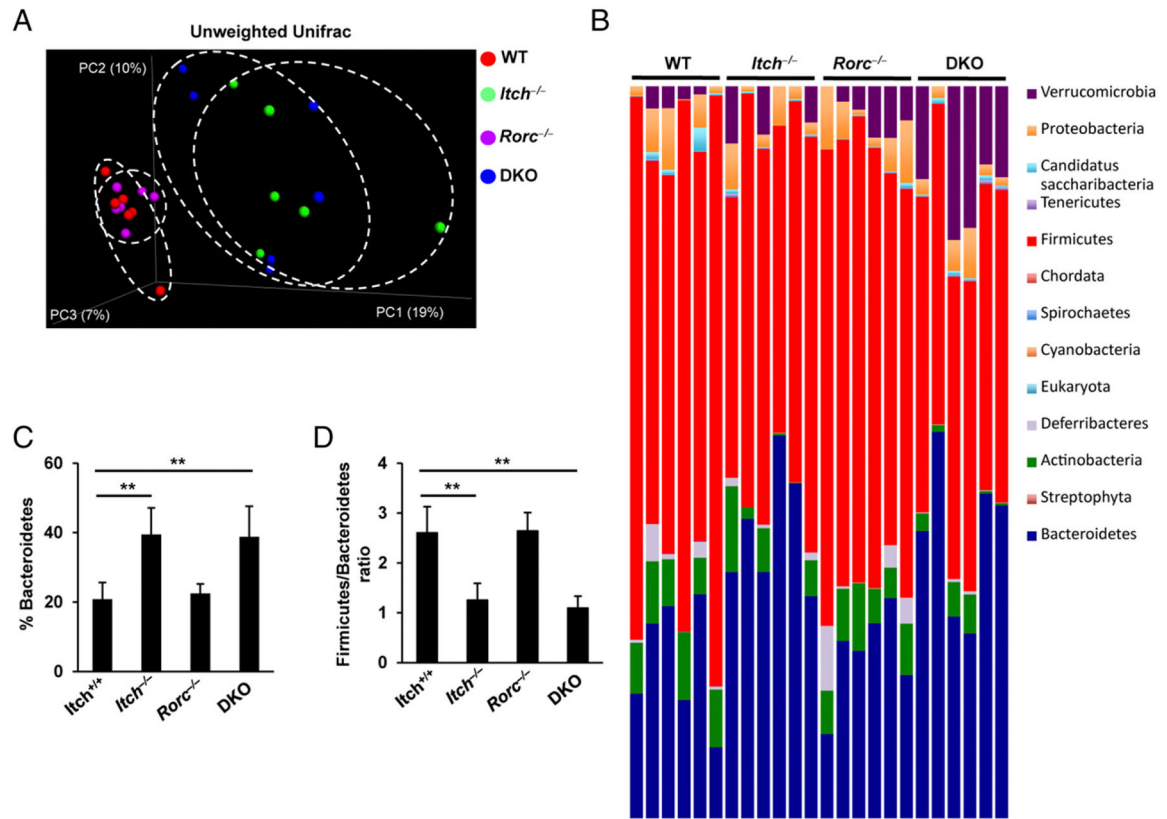
Antibiotic treatment reduces spontaneous colon inflammation in *Itch*^{-/-} mice. (A) Representative images of H&E-stained colon sections of *Itch*^{-/-} and *Itch*^{-/-} treated with an antibiotic mixture are shown along with histology score. Images were taken at original magnification $\times 10$. (B–D) RNA isolated from *Itch*^{+/+}, *Itch*^{-/-}, and *Itch*^{-/-} mice after antibiotic treatment and assayed by RT-PCR showed significant differences between the *Itch*^{-/-} and antibiotic-treated *Itch*^{-/-} groups in expression of (B) IL-17A and IL-17F, (C) chemokines, and (D) MMPs. Data represent mean \pm SD. ** $p < 0.01$.

**FIGURE 3.**

Reconstitution of *Itch*^{-/-} microbiota in *Itch*^{+/+} mice does not induce spontaneous colon inflammation. *Itch*^{-/-} microbiota was reconstituted in *Itch*^{+/+} mice, and 16S rRNA sequencing of fecal pellets was performed. The relative abundance of phylum-classified fecal microbiota differed between the groups, as shown in (A) histograms based on the proportion of OTUs per subject. (B) Differences were also seen in the unweighted UniFrac distance principal coordinate analysis of the fecal microbiota from 7 *Itch*^{+/+} (red dots), 7 *Itch*^{-/-} (blue dots), and 7 *Itch*^{+/+} gavaged *Itch*^{-/-} microbiota (green dots). (C) Changes in microbiota as measured by the Θ YC distance. (D) H&E staining of colon sections of *Itch*^{+/+} mice reconstituted with *Itch*^{-/-} microbiota showed no morphological changes. Images were taken at original magnification $\times 10$. (E) Histology score. (F and G) RNA isolated from *Itch*^{+/+} and *Itch*^{+/+} mice after reconstitution of microbiota showed no significant differences between the groups in expression of (F) IL-17A and IL-17F or (G) IL-6, TNF- α , and IL-1 β by RT-PCR. Data represent mean \pm SD. ***p* < 0.01. ns, not significant.

**FIGURE 4.**

Reconstitution of Itch^{-/-} microbiota in Itch^{+/+} mice makes them more susceptible to DSS-induced colitis. Itch^{+/+} ($n = 6$), Itch^{-/-} ($n = 6$), and Itch^{+/+} mice given Itch^{-/-} microbiota ($n = 6$) were given 2.5% DSS solution for 5 d followed by 3 d of water. Mice were sacrificed on day 8. Significant differences between groups were seen in some daily recordings of (A) body weight, (B) diarrhea score, and (C) FOB, as well as in (D) histology scores. Data represent mean \pm SD. * $p < 0.05$, ** $p < 0.01$.

**FIGURE 5.**

Itch^{-/-} *Rorc*^{-/-} DKO mice have altered gut microbiota. Results from 16S rRNA sequencing of fecal pellets from *Itch*^{+/+} and *Itch*^{-/-} mice, showing (A) unweighted UniFrac distance principal coordinate analysis of the fecal microbiota from 6 *Itch*^{+/+} (red dots), 6 *Itch*^{-/-} (green dots), 6 *Rorc*^{-/-} (purple dots), and 6 *Itch*^{-/-}*Rorc*^{-/-} DKO mice (blue dots). (B) Relative abundance of phylum-classified fecal microbiota; (C) Percentage of *Bacteroidetes* present in fecal microbiota from *Itch*^{+/+}, *Itch*^{-/-}, *Rorc*^{-/-}, and *Itch*^{-/-}*Rorc*^{-/-} DKO mice. (D) *Bacteroidetes*-to-*Firmicutes* ratio in fecal microbiota from *Itch*^{+/+} and *Itch*^{-/-} mice. Data represent mean ± SD. ***p* < 0.01.

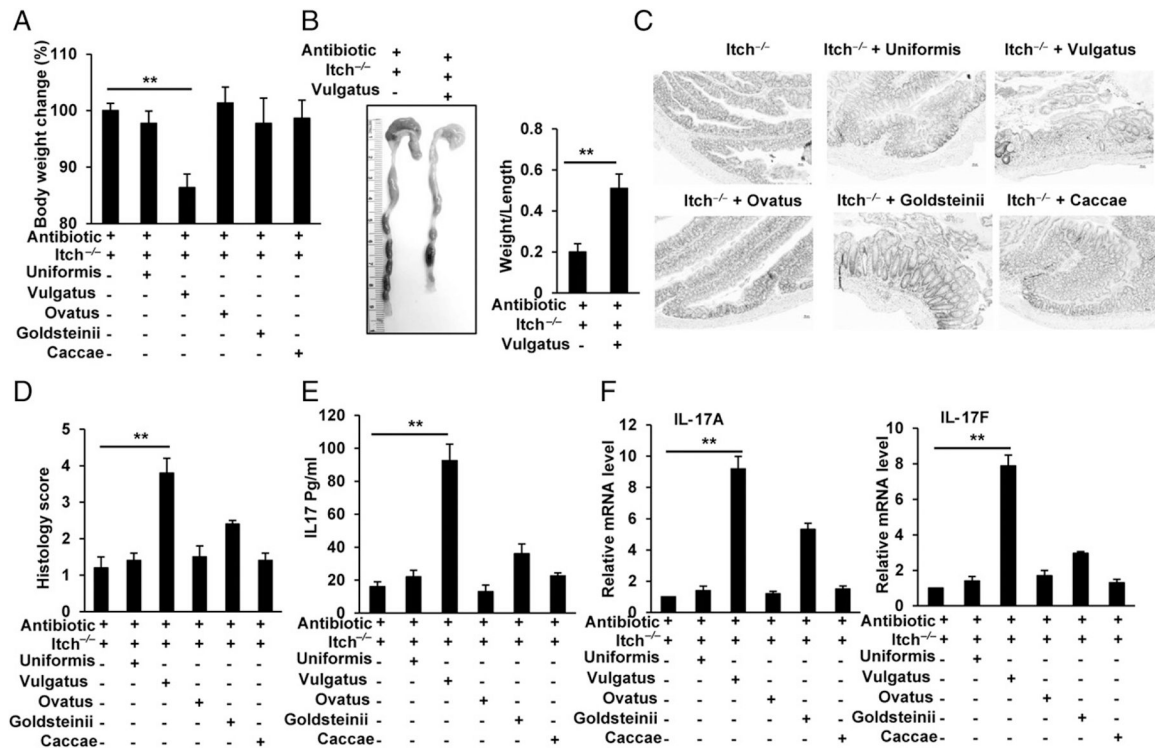


FIGURE 6. *Bacteroides vulgatus* induces colon inflammation in Itch^{-/-} mice. Antibiotic-pretreated Itch^{-/-} were gavaged with different *Bacteroides* strains (five mice per strain). Results show (A) percentage body weight change at the end of the experiment and (B) representative images of colons from Itch^{-/-} and Itch^{-/-} mice gavaged with *B. vulgatus* with weight/length ratio. (C) H&E staining of colon sections of Itch^{-/-} mice gavaged with different *Bacteroides* strains. Images were taken at original magnification $\times 10$. (D) Histology score of Itch^{-/-} and Itch^{-/-} mice gavaged with different *Bacteroides* strains. (E) IL-17A ELISA from the colon tissue explant of Itch^{-/-} and Itch^{-/-} mice gavaged with different *Bacteroides* strains, and (F) RT-PCR of IL-17A and IL-17F from colon tissue of Itch^{-/-} and Itch^{-/-} mice gavaged with different *Bacteroides* strains. ** $p < 0.01$.